IAI Journals.ASM.org

Titan Cell Production Enhances the Virulence of *Cryptococcus neoformans*

Juliet N. Crabtree,[a] Laura H. Okagaki,[a] Darin L. Wiesner,[a] Anna K. Strain,[a] Judith N. Nielsen,[b] and Kirsten Nielsen[a]

Department of Microbiology, Medical School, University of Minnesota, Minneapolis, Minnesota, USA,[a] and Department of Pathology and Laboratory Medicine, School of Medicine, University of North Carolina at Chapel Hill, Chapel Hill, North Carolina, USA[b]

Infection with *Cryptococcus neoformans* begins when desiccated yeast cells or spores are inhaled and lodge in the alveoli of the lungs. A subset of cryptococcal cells in the lungs differentiate into enlarged cells, referred to as titan cells. Titan cells can be as large as 50 to 100 μm in diameter and exhibit a number of features that may affect interactions with host immune defenses. To characterize the effect of titan cell formation on the host-pathogen interaction, we utilized a previously described *C. neoformans* mutant, the *gpr4*Δ *gpr5*Δ mutant, which has minimal titan cell production *in vivo*. The *gpr4*Δ *gpr5*Δ mutant strain had attenuated virulence, a lower CFU, and reduced dissemination compared to the wild-type strain. Titan cell production by the wild-type strain also resulted in increased eosinophil accumulation and decreased phagocytosis in the lungs compared to those with the *gpr4*Δ *gpr5*Δ mutant strain. Phagocytosed cryptococcal cells exhibited less viability than nonphagocytosed cells, which potentially explains the reduced cell survival and overall attenuation of virulence in the absence of titan cells. These data show that titan cell formation is a novel virulence factor in *C. neoformans* that promotes establishment of the initial pulmonary infection and plays a key role in disease progression.

Cryptococcus neoformans is an opportunistic fungal pathogen that causes meningoencephalitis in severely immunocompromised individuals, including people living with HIV/AIDS. Current epidemiological estimates show that fatalities due to cryptococcosis exceed 650,000 each year in people with AIDS (37). In sub-Saharan Africa, cryptococcosis has now surpassed tuberculosis in terms of annual fatality rates (37). Thus, cryptococcosis is emerging as a significant disease in immunocompromised populations worldwide, with particularly high burdens of disease in the developing world, where access to quality medical care is limited.

The infectious particles are thought to be spores, although desiccated yeast cells are also small enough to be inhaled and then lodge in the alveoli of the lungs (19). Upon inhalation into the lungs, spores germinate to produce yeast cells that can establish the initial pulmonary infection (5, 19). The pulmonary infection is typically controlled or cleared in healthy individuals. However, in immunocompromised individuals, the infection can disseminate from the lungs, penetrate the blood-brain barrier, and result in highly lethal meningitis (5, 19).

Several virulence factors, such as capsule and melanin, produced by *C. neoformans* during the infectious process, have been shown to promote survival in the host. Capsule plays a critical role in modulation of the host immune system through sequestration of opsonins such as antibodies and complement C3, as well as by induction of host phagocytic cell apoptosis (19, 26, 43). Acapsular mutant strains are avirulent in animal models of cryptococcosis (1, 6–10, 19). Protection from oxidative and nitrosative stresses generated by host phagocytes and neutrophils is conferred by the dark pigment melanin (19). Synthesis of melanin is regulated by laccase (LAC) genes, and *lac1*Δ mutant strains have attenuated virulence in animal models (19, 28, 31, 38–40). Additional virulence factors, such as urease and hyaluronic acid production, affect survival within macrophages or direct interactions with the endothelial cells of the blood-brain barrier (22, 23, 35). Thus, *C. neoformans* has evolved multiple strategies to evade host defenses against infection.

A novel cell morphology was recently characterized for cryptococcal pulmonary infections that may promote pulmonary survival and dissemination. Upon exposure to the pulmonary environment, a subset of cryptococcal cells in the lungs produce enlarged "titan" cells (33, 46). Approximately 10 to 20% of the cryptococcal cells in the lungs transition to the titan cell phenotype and grow to be as large as 50 to 100 μm in diameter, which is 5- to 10-fold larger than a typical cryptococcal cell (33).

Titan cells have several characteristics that differentiate them from normal-size cells. First, titan cells have an altered capsule structure which is highly cross-linked and cannot be sheared from the cryptococcal cell by chemical or physical methods (46). Second, the cell wall of titan cells is approximately 30- to 50-fold thicker than the cell wall of normal-size cells, as seen by transmission electron microscopy (TEM) (46). Third, titan cells are resistant to oxidative and nitrosative stresses similar to those employed by phagocytes to kill pathogens (33, 46). Finally, titan cells are too large to be phagocytosed by host immune cells in the lungs, and the production of titan cells reduces phagocytosis of normal-size cryptococcal cells (32). Taken together, these data show that titan cells have characteristics that may promote survival *in vivo*.

The known characteristics of titan cells suggest that their production could be important for cryptococcal virulence. To test this hypothesis, we analyzed the survival and virulence of purified

Received 14 May 2012 **Returned for modification** 1 June 2012
Accepted 2 August 2012
Published ahead of print 13 August 2012
Editor: G. S. Deepe, Jr.
Address correspondence to Kirsten Nielsen, knielsen@umn.edu.
J.N.C. and L.H.O. contributed equally to this article.
Supplemental material for this article may be found at http://iai.asm.org/.

doi:10.1128/IAI.00507-12

titan cells as well as mutant strains with altered titan cell production. We show that titan cell production promotes survival in the host and enhances cryptococcal virulence. These data show that titan cell production is a virulence factor in *C. neoformans*.

MATERIALS AND METHODS

Animal experiments. All animals were handled in strict accordance with good animal practice as defined by the relevant national and local animal welfare bodies, i.e., (i) the University of Minnesota Institutional Animal Care and Use Committee (IACUC), under protocol numbers 0712A22250 and 1010A91133; and (ii) the University of North Carolina-Chapel Hill IACUC, under protocol number 09-166.0. Mice used for this study were female C57BL/6 and A/J mice (Jackson Laboratory, Bar Harbor, ME) between the ages of 6 and 8 weeks. All mice were housed in AAALAC-accredited animal facilities with approved Public Health Service (PHS) assurance.

Strains and media. Strains of *Cryptococcus neoformans* var. *grubii* used in this study were KN99α (wild type) (30), CDX18 (*gpr4*Δ *gpr5*Δ) (34, 45), LHO31-1 (*otc1*Δ) (32), and LHO17 (*gpr4*Δ *GPR5*). The LHO17 strain was isolated from the progeny of matings between CDX18 and KN99**a**. Briefly, matings were performed on V8 agar, and basidiospores were micromanipulated as previously described (20). The *gpr4*Δ *GPR5* strain was isolated using yeast extract-peptone-dextrose (YPD) agar containing 200 μg/ml neomycin (NEO) and via a lack of growth on YPD agar containing 200 μg/ml nourseothricin (NAT). Strains were then screened by PCR to verify the presence of wild-type GPR5 and to determine the mating type. All strains were stored in glycerol at −80°C and grown on YPD agar or in YPD broth medium (BD Biosciences, Sparks, MD).

Growth assays. To assess whether the mutant strains had altered growth phenotypes *in vitro*, liquid cultures of KN99α, the *gpr4*Δ *gpr5*Δ strain, the complemented *gpr4*Δ *GPR5* strain, and the *otc1*Δ strain were inoculated and allowed to grow overnight in YPD. Stationary-phase cultures were serially diluted 1:40 in phosphate-buffered saline (PBS; Lonza, Rockland, ME) and then 1:50 in four different growth media: YPD, Dulbecco's modified Eagle's medium (DMEM; Life Technologies, Grand Island, NY) supplemented with 10% fetal bovine serum (FBS; ATCC, Manassas, VA), and L-DOPA medium with and without L-3,4-dihydroxyphenylalanine (DOPA). Two 96-well round-bottom plates were inoculated with triplicate cultures of each strain in 150 μl of each medium. Each plate was incubated for 48 h with shaking in a Tecan Sunrise plate reader (Tecan Group Ltd., Männedorf, Switzerland), and the absorbance at 595 nm was measured every 15 min. One plate was grown at 30°C, and one was grown at 37°C. *In vitro* growth assays were performed twice, with similar results. Additional growth assays were performed in which 1×10^6 cells of each strain were serially diluted, spotted onto YPD medium, and grown at either 30°C or 37°C.

To assess *in vivo* replication, *C. neoformans* cells were cultured overnight in YPD broth. The resulting yeast cells were labeled with Alexa Fluor 488 (AF488) or Alexa Fluor 594 (AF594) (Invitrogen, Grand Island, NY) as described previously (33), pelleted, and resuspended in sterile PBS at a concentration of 1×10^8 cells/ml, based on hemacytometer counts. Groups of 6- to 8-week-old female C57BL/6 mice were anesthetized by intraperitoneal pentobarbital injection. Three to five mice per treatment were infected intranasally with 5×10^6 cells in 50 μl PBS. At 3 days postinfection, mice were sacrificed by CO_2 inhalation. Lungs were subjected to lavage with 1.5 ml sterile PBS three times, using an 18.5-gauge needle placed in the trachea. Cells in the lavage fluid were pelleted at 16,000 × *g*, resuspended in 3.7% formaldehyde, and incubated at room temperature for 30 min. Cells were then washed once with PBS, and >2,000 cells per animal were examined by microscopy (AxioImager; Carl Zeiss, Inc.). Ratios of stained cells (original inoculum) to unstained cells (nascent cells) were used to calculate *in vivo* doubling times.

To assess whether mutant strains have altered growth in whole blood, C57BL/6 mice were euthanized by CO_2 inhalation. Whole blood was collected by cardiac puncture, and heparin sodium (Sigma, St. Louis, MO) was added as an anticoagulant to a final concentration of 50 μg/ml of blood. KN99α (wild-type) and CDX18 (*gpr4*Δ *gpr5*Δ) cells were cultured overnight on YPD agar. The resulting yeast cells were resuspended in sterile PBS to a concentration of 1×10^6 cells/ml by hemacytometer count. A total of 1×10^4 cells were added to 100 μl whole blood with 50 μg/ml heparin sodium, YPD broth with 50 μg/ml heparin sodium, or YPD broth. Samples were incubated for 24 h at 37°C and 5% CO_2. Serial dilutions were plated on YPD agar for CFU enumeration.

Analysis of virulence factor production. The *gpr4*Δ *gpr5*Δ and *otc1*Δ mutant strains as well as the wild-type KN99α strain were grown overnight in YPD broth at 30°C. Ten microliters of each culture was spotted onto Christensen's urea agar medium (13) or L-DOPA medium (12) to test urease or melanin production, respectively. Plates were incubated at 30°C and monitored daily for a pH change (Christensen's urea medium) or melanin pigmentation (L-DOPA medium). In addition, urease, melanin, and *in vitro* capsule production was quantified following broth culture by use of an H1 Synergy plate reader (BioTek Instruments Inc., Winooski, VT). Samples were prepared as described above for growth assays, with the inclusion of Christensen's urea medium, and the absorbances at 560 nm (urease) and 350 nm (melanin) were determined. *In vitro* capsule production was measured using a Premier cryptococcal antigen kit (Meridian Bioscience, Cincinnati, OH). Capsule production was also analyzed *in vivo*. Briefly, cells were cultured overnight in YPD broth, pelleted, and resuspended in sterile PBS, and mice were infected intranasally with 5×10^6 cells in 50 μl PBS. At 3 days postinfection, mice were sacrificed by CO_2 inhalation. Lungs were subjected to lavage, cells in the lavage fluid were fixed and stained with India ink, and the capsule was observed by microscopy.

Purified titan and normal-size cells. KN99α and KN99**a** cells were cultured overnight in YPD broth. The resulting yeast cells were pelleted and resuspended in sterile PBS. To harvest titan cells, A/J or C57BL/6 mice were anesthetized by intraperitoneal pentobarbital injection and infected intranasally with 5×10^6 KN99α cells, or a 1:1 ratio of KN99α and KN99**a** cells to stimulate titan cell production, in 50 μl PBS. At 3 or 5 days postinfection, mice were sacrificed by CO_2 inhalation and lungs subjected to lavage as described above. Cells in the bronchoalveolar lavage (BAL) fluid were pelleted, resuspended in 0.05% SDS in sterile water for 1 min to promote host cell lysis, pelleted, and resuspended in PBS. Titan and normal-size cells were purified using fluorescence-activated cell sorting (FACS) or by filtration. For FACS, cells were sorted based on size, using an iCyt Reflection flow cytometer (iCyt, Champaign, IL). Because capsule size differences can affect cell size analysis by forward scatter during flow cytometry, normal-size cells were classified as those with a cell body diameter of ≤10 μm, and titan cells were classified as those with a cell body diameter of ≥15 μm. After sorting, the titan cell population had >97% purity and the normal-size cell population had >90% purity. For filtration purification, titan cells were isolated by filtration through a 20-μm CellMicroSieve (BioDesign, New York, NY), concentrated by centrifugation, and resuspended in sterile PBS. Normal-size cells that passed through the filter were concentrated by centrifugation and resuspended in sterile PBS. To infect mice with the purified cell populations, groups of A/J or C57BL/6 mice were anesthetized and infected intranasally with 1×10^3 or 1×10^4 purified titan or normal-size cells in 25 or 50 μl of PBS. Mice were sacrificed at 3, 5, and 7 days postinfection. Lungs from each animal were homogenized in 1 or 4 ml PBS, and serial dilutions were plated on YPD agar for CFU enumeration.

Survival assay. Ten C57BL/6 mice per group were anesthetized and inoculated intranasally with 1×10^3 wild-type KN99α, *gpr4*Δ *gpr5*Δ, or *gpr4*Δ *GPR5* cells suspended in 50 μl PBS. Animals were monitored for morbidity and sacrificed when endpoint criteria were reached. Endpoint criteria were defined as 20% total body weight loss, loss of 2 grams of weight in 2 days, or symptoms of neurological damage. Tissues (lung and brain) were collected from a subset of animals to determine fungal burdens at the time of sacrifice. Mice that survived to 62 days postinfection

without exhibiting signs of disease were sacrificed and their tissues processed as described above for determination of fungal burdens.

***In vivo* growth kinetics.** Overnight broth cultures of wild-type KN99α, *gpr4*Δ *gpr5*Δ, or *otc1*Δ cells were pelleted, washed with sterile PBS, and resuspended to 2×10^4 cells/ml based on hemacytometer counts. Eight C57BL/6 mice per strain per time point were anesthetized, and 1×10^3 cells in 50 μl of inoculum was administered intranasally. Mice were sacrificed either at 0, 6, 14, 24, and 30 h postinfection or at 0, 5, 7, 14, and 21 days postinfection. Lungs, spleens, and brains were collected in 1 ml sterile PBS, homogenized, and plated on YPD agar supplemented with chloramphenicol for enumerating CFU.

Intracerebral infections. Animals were deeply anesthetized by intraperitoneal injection of pentobarbital. Eight C57BL/6 mice per group were infected intracerebrally with 1×10^3 fungal cells in 20 μl PBS injected slowly into the top of the cerebrum. At 4 days postinfection, animals were sacrificed, and brains were collected, processed as described above, and plated for CFU.

Phagocytosis viability assay. Cryptococcal cells were fluorescently labeled using an Alexa Fluor 488 protein labeling kit (Invitrogen, Eugene, OR) as described above. C57BL/6 mice were anesthetized and inoculated intranasally with 5×10^6 labeled cells in 50 μl PBS. At 24 h postinfection, mice were sacrificed and BAL was performed. Three or four lavage fluid samples were pooled, pelleted at 376 × *g* for 5 min, resuspended in 100 μl FACSBuffer (PBS plus 2% fetal bovine serum), and stained with anti-CD45–allophycocyanin (APC) (BioLegend, San Diego, CA) at a 1:100 dilution. Cells were stained on ice in the dark for 30 min, washed three times with FACSBuffer, and resuspended in FACSBuffer for sorting on a FACS Aria II flow cytometer (BD Biosciences, Sparks, MD). Double-positive ($AF488^+$ APC^+) cells were defined as phagocytosed cryptococcal cells, and single-positive ($AF488^+$ APC^-) cells were defined as extracellular cryptococcal cells. After sorting, the cell number collected by the FACS Aria II instrument was recorded, and serial dilutions were plated on YPD agar to assess viability. For a subset of studies, the cell number collected during sorting was verified by hemacytometer counts. Percent survival was calculated by dividing the number of CFU by the total number of cells plated for each sample.

Lung leukocyte isolation. Lung leukocytes were isolated as described previously (47). Briefly, lungs were excised, placed in Hanks balanced salt solution (HBSS) with 1.3 mM EDTA, and minced to generate approximately 1-mm^3 pieces. The lung mince was then incubated in the HBSS–1.3 mM EDTA solution for 30 min at 37°C with agitation. The cells were pelleted, resuspended in RPMI medium supplemented with 5% FBS and 150 U/ml type I collagenase (Invitrogen, Grand Island, NY), and incubated for 1 h at 37°C with agitation. The cells were passed through a 70-μm filter, pelleted, resuspended in 44% Percoll-RPMI medium (GE Life Sciences, Pittsburgh, PA), and added to a Percoll density gradient (44% top, 67% bottom), and the samples were centrifuged for 20 min at 650 × *g*. The leukocytes at the interface were removed, washed 2 times with 10 ml of RPMI medium, and resuspended in medium at a concentration of 10^7 cells/ml.

Leukocytes were processed for flow cytometry by treatment with CD16/32 antibody to block the FC receptor and prevent nonspecific antibody binding. Cells were stained with Siglec-F–phycoerythrin (BD Biosciences, San Jose, CA), IgE-fluorescein isothiocyanate, Ly6G-allophycocyanin-eFluor 780, and phycoerythrin-cyanine 5 (eBiosciences, San Diego, CA) at a 1:100 dilution. For data acquisition, >250,000 events were collected on a BD FACSCanto II flow cytometer (BD Biosciences, San Jose, CA), and the data were analyzed with FlowJo 8.7 (Tree Star Inc., Ashland, OR).

Eosinophils were identified as described previously (41, 48), with the following modifications. Live cells were gated based on forward and side scatter properties. Eosinophils were identified as Siglec-F-positive, IgE-negative, Ly6G-intermediate, and CD11c-negative cells. Figure S4 in the supplemental material depicts the gating strategy used to identify and quantify the eosinophil population.

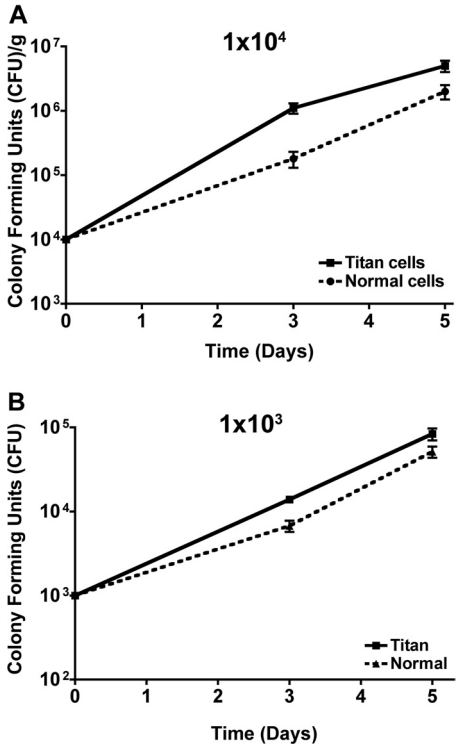

FIG 1 Infections with purified titan cells result in larger lung fungal burdens. (A) A/J mice were infected intranasally with 1×10^4 wild-type (KN99α) titan or normal-size cells purified by cell sorting. (B) C57BL/6 mice were infected intranasally with 1×10^3 wild-type (KN99α) titan or normal-size cells purified by filtration. Lungs were extracted at 3 and 5 days postinfection and homogenized, and serial dilutions were plated to determine tissue burdens. Error bars indicate standard deviations for 4 or 5 mice per time point.

Statistical analysis. All statistical analyses were performed using GraphPad Prism (GraphPad Software, Inc., San Diego, CA) or Analyze-It (Analyze-It, Ltd., Leeds, United Kingdom). The Mann-Whitney U test was used to analyze survival, intracerebral infections, phagocytosis viability assays, and brain and lung CFU from survival assays. One-way analysis of variance (ANOVA) was used to analyze differences in doubling times. Two-way ANOVA was used to analyze *in vivo* growth curves for the lung, spleen, and brain. *P* values of <0.05 were considered significant.

RESULTS

Purified titan cells accumulate faster than normal-size cells during early pulmonary infection. Titan cells are generated in response to the pulmonary environment and have characteristics that may promote their survival (32, 33, 46). These observations suggest that titan cell production may provide a growth advantage during establishment of pulmonary infection. To test this hypothesis, FACS and filtration were used to purify wild-type titan or normal-size cells from *in vivo* samples. The purified populations were enriched >90% by FACS or filtration. Control infections with normal-size cells grown *in vitro* or isolated from *in vivo* samples by FACS or filtration showed no differences in fungal burdens measured by CFU at 3, 5, or 7 days postinfection, showing that FACS did not alter the viability of the cells (data not shown).

Mice infected with purified titan cells had higher CFU at 3 and 5 days postinfection than did mice infected with purified normal-size cells (Fig. 1). At 3 days postinfection, mice infected with purified titan cells had a significant increase in fungal burden com-

pared to mice infected with normal-size cells (Fig. 1) ($P = 0.015$ and $P = 0.0079$ for mice infected with 1×10^4 cells and 1×10^3 cells, respectively). This increase in fungal burden was still significant at 5 days postinfection for mice infected with 1×10^4 cells (Fig. 1A) ($P = 0.043$) but was no longer statistically significant for mice infected with 1×10^3 cells (Fig. 1B) ($P = 0.29$). These data indicate that titan cells can provide a growth advantage during establishment of pulmonary infection.

By 7 days postinfection, equivalent CFU were observed in mice infected with purified titan cells or normal-size cells at both the higher and lower inoculums ($P = 0.89$ and $P = 0.56$, respectively) (data not shown). Previous studies showed that normal-size cryptococcal cells can develop into titan cells within 24 h and that titan cells generate normal-size cells upon budding (33, 46). Analysis of the cryptococcal cells in the lungs of mice infected with the purified cell populations at 7 days postinfection revealed a mixture of both normal-size and titan cells (data not shown). Thus, the purified populations were not maintained over time, and the long-term effects on fungal burden due to titan cell production could not be determined using these FACS- or filter-purified cell populations.

Titan cell production enhances virulence in murine survival assays. To determine the long-term effects of titan cell formation on the virulence of *C. neoformans*, a system in which the titan cell and normal-size cell states were maintained over time was needed. A targeted mutant screen was performed to identify genes involved in titan cell development that did not alter other traits known to affect virulence (34). This screen showed that the *gpr4*Δ *gpr5*Δ mutant, which lacks both the Gpr4 and Gpr5 receptors, important for environmental sensing, had significantly reduced titan cell formation (34, 45). While the wild-type strain exhibited 20% titan cell production at 72 h postinfection, the *gpr5*Δ and *gpr4*Δ *gpr5*Δ mutant strains exhibited 3% and <1% titan cell formation, respectively (32, 34). Deletion of *GPR4* alone (*gpr4*Δ) did not affect titan cell production, but lack of this gene further reduced titan cell production in the *gpr4*Δ *gpr5*Δ mutant (32, 34). Complementation of the *GPR5* gene restored titan cell formation in the *gpr4*Δ *GPR5* strain to wild-type levels (32, 34).

To utilize the *gpr4*Δ *gpr5*Δ strain in assays to determine the effect of titan cell production on cryptococcal survival and virulence in the host, we determined whether the *gpr4*Δ *gpr5*Δ strain had altered production of other factors known to affect virulence. The *gpr4*Δ *gpr5*Δ strain exhibited wild-type growth and cell size in DMEM, minimal medium, and rich medium, at both 30°C and 37°C (see Fig. S1 in the supplemental material; also data not shown). In addition, the *in vivo* replication rates for the wild-type and *gpr4*Δ *gpr5*Δ strains were determined by monitoring cell division of fluorescently labeled cells and quantifying the proportion of the population that was no longer fluorescent (see Table S1). The *in vivo* replication rates for the wild-type and *gpr4*Δ *gpr5*Δ strains were equivalent ($P = 0.44$). Finally, the *gpr4*Δ *gpr5*Δ strain expressed wild-type levels of other virulence factors, including capsule, melanin, and urease (see Fig. S2; also data not shown). Thus, the *gpr4*Δ and *gpr5*Δ mutations do not have global effects on virulence factor production. While we cannot rule out the possibility that the *gpr4*Δ *gpr5*Δ strain has a defect in an as yet uncharacterized phenotype important for virulence, the mutations appear to affect titan cell production only.

The *gpr4*Δ *gpr5*Δ strain, with limited titan cell production, was used to assess the long-term effect of titan cell production on the survival and proliferation of *C. neoformans* in the murine inhalational model of cryptococcosis. We hypothesized that titan cell production would promote *C. neoformans* virulence and that the *gpr4*Δ *gpr5*Δ strain, with reduced titan cell production, would have attenuated virulence. To test this hypothesis, mice were infected intranasally with the wild-type, *gpr4*Δ *gpr5*Δ, or complemented *gpr4*Δ *GPR5* strain and monitored for signs of morbidity (Fig. 2). All mice infected with the wild-type strain succumbed to the infection between 21 and 27 days postinfection (Fig. 2). In contrast, mice infected with the *gpr4*Δ *gpr5*Δ mutant strain did not exhibit morbidity until 28 days postinfection, and only 40% of mice succumbed to the infection by 61 days postinfection (Fig. 2) ($P = 0.0001$). The complemented *gpr4*Δ *GPR5* strain had virulence equivalent to that of the wild-type strain in this survival assay (Fig. 2) ($P = 0.53$). Thus, the attenuated virulence observed in the *gpr4*Δ *gpr5*Δ strain was due to deletion of the *GPR5* gene.

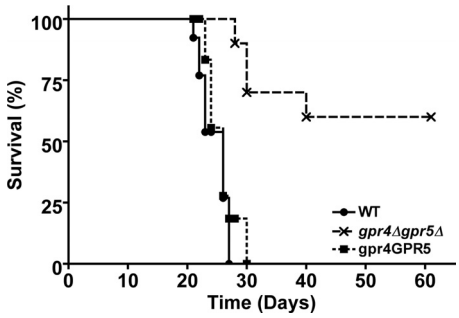

FIG 2 Titan cell production enhances virulence of *C. neoformans*. Groups of 10 C57BL/6 mice were infected intranasally with 1×10^3 wild-type (KN99α; WT), *gpr4*Δ *gpr5*Δ, or *gpr4*Δ *GPR5* cells, and progression to severe morbidity was monitored for 62 days.

Mice that succumbed to the *gpr4*Δ *gpr5*Δ infection exhibited lower fungal burdens in the lungs than those of mice infected with the wild-type strain, whereas fungal burdens in the brain were equivalent between the two strains (Fig. 3) ($P = 0.036$ and $P = 0.79$, respectively). These data show that the 40% mortality observed with the *gpr4*Δ *gpr5*Δ infections was due to central nervous system (CNS) disease. Mice that did not succumb to the *gpr4*Δ *gpr5*Δ infection by 62 days postinfection had low lung and brain fungal burdens (Fig. 4), suggesting that 60% of the mice had controlled the *gpr4*Δ *gpr5*Δ infection. Taken together, these data show that reduced titan cell formation resulted in attenuated virulence.

Titan cell production enhances pulmonary survival and proliferation. The initial site of cryptococcal infection is the lungs. Based on infections with wild-type purified titan cell populations, we hypothesized that titan cells may promote establishment of the pulmonary infection. Therefore, we determined the effects of titan cell production on the pulmonary fungal burden by using the *gpr4*Δ *gpr5*Δ mutant strain. Mice were infected intranasally with wild-type or *gpr4*Δ *gpr5*Δ cells, and CFU in the lungs were determined at 0, 6, 14, 24, and 30 h as well as at 5, 7, 14, and 21 days postinfection (Fig. 5). Both the wild-type and *gpr4*Δ *gpr5*Δ strains had lower CFU in the lungs at 6 h postinfection than at the baseline (0 h) time point (Fig. 5A), suggesting cryptococcal cell death upon exposure to the pulmonary environment. While the difference in fungal burdens at 6 h was not statistically significant, the trend was consistent between multiple experiments. The *gpr4*Δ *gpr5*Δ mutant strain, lacking titan cell production, exhibited re-

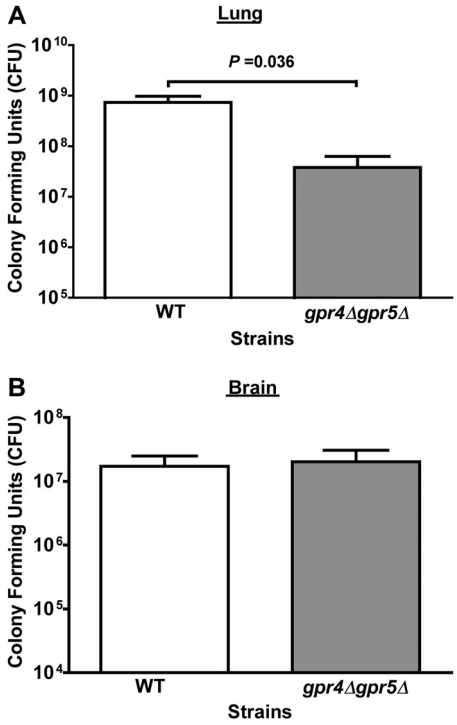

FIG 3 Fungal burdens in mice that succumbed to infection with wild-type or *gpr4*Δ *gpr5*Δ strain. C57BL/6 mice were infected intranasally with 1×10^3 wild-type (KN99α) or *gpr4*Δ *gpr5*Δ cells, monitored for disease morbidity, and sacrificed when endpoint morbidity criteria were reached. Lungs (A) and brains (B) were harvested and homogenized, and serial dilutions were plated for CFU determinations. Error bars indicate standard deviations for 3 to 5 mice per treatment group.

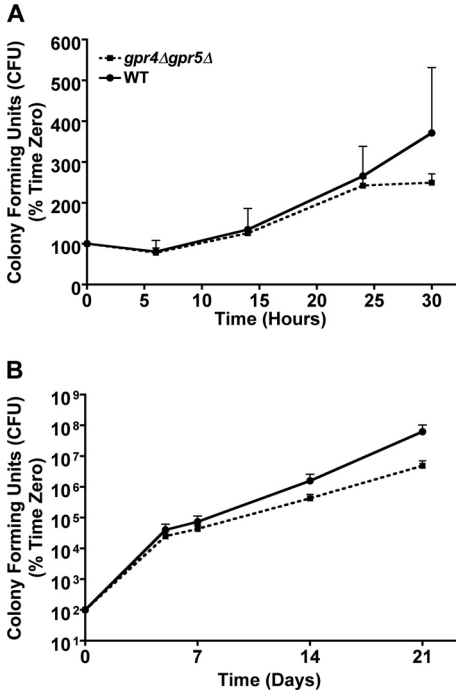

FIG 5 Titan cell production enhances survival and proliferation in the pulmonary environment. C57BL/6 mice were infected intranasally with 1×10^3 wild-type (KN99α) or *gpr4*Δ *gpr5*Δ cells. At 0, 6, 14, 24, and 30 h postinfection (A) or 0, 5, 7, 14, and 21 days postinfection (B), lungs were harvested and homogenized, and serial dilutions were plated to determine tissue burdens. Fungal burdens are expressed as percentages relative to the level at 0 h postinfection. Error bars represent standard deviations for 7 or 8 mice per strain per time point.

duced fungal burdens compared to those of the wild-type strain by 30 h postinfection (Fig. 5A). This trend continued throughout the infection. By 21 days postinfection, the *gpr4*Δ *gpr5*Δ mutant strain had a 10-fold reduction in CFU compared to the wild-type strain (Fig. 5B) ($P = 0.001$). The observation that lower fungal burdens were seen in the absence of titan cell production suggests that production of titan cells promotes survival and proliferation of cryptococcal cells in the pulmonary environment.

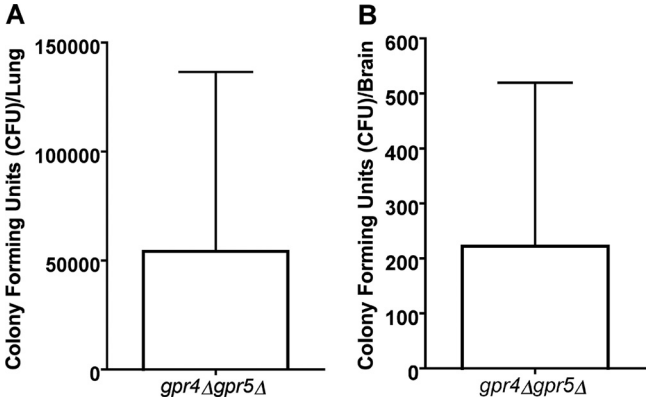

FIG 4 Fungal burdens in mice that survived infection with the *gpr4*Δ *gpr5*Δ strain. C57BL/6 mice were infected intranasally with 1×10^3 *gpr4*Δ *gpr5*Δ cells and monitored for 62 days. Those animals that survived to 62 days without signs of disease morbidity were sacrificed, lungs (A) and brains (B) were harvested and homogenized, and serial dilutions were plated for CFU determinations. Error bars indicate standard deviations for 5 mice.

Consistent with these findings, an *otc1*Δ mutant that overproduces titan cells (32) had enhanced survival in the pulmonary environment (see Fig. S3 in the supplemental material). The *otc1*Δ strain has a mutation in the *OTC1* gene, encoding a protein of unknown function (32). Similar to the *gpr4*Δ *gpr5*Δ strain, the *otc1*Δ strain exhibited wild-type *in vitro* growth and expression of other factors important for virulence (see Fig. S1 and S2; also data not shown). However, the *otc1*Δ strain had impaired *in vivo* replication (see Table S1). Even in the absence of *in vivo* replication, the titan cell-overproducing *otc1*Δ strain resisted the initial cell death observed in the wild-type and *gpr4*Δ *gpr5*Δ strains (data not shown). In addition, the *otc1*Δ titan cells persisted in the lungs for at least 62 days postinfection (see Fig. S3B). No dissemination of the *otc1*Δ mutant strain overproducing titan cells was observed (see Fig. S3C). These data suggest that titan cell production can promote cryptococcal cell survival upon exposure to the pulmonary environment, even in the absence of cell division.

Titan cell production inhibits phagocytosis to promote *C. neoformans* survival. Phagocytosis by resident alveolar macrophages is one of the first lines of defense utilized by the innate immune system to control pulmonary infections (4). Previous studies have shown that titan cells are resistant to phagocytosis and that titan cell production significantly decreases the pulmonary phagocytosis rate of *C. neoformans* (32, 33). The data presented above show that titan cell production resulted in increased

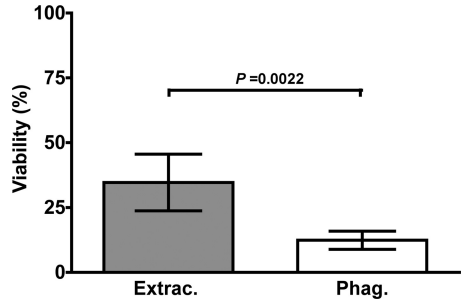

FIG 6 Extracellular cryptococcal cells have higher viability than phagocytosed cells. C57BL/6 mice were infected intranasally with 5×10^6 KN99α or *gpr4*Δ *gpr5*Δ cells labeled with Alexa Fluor 488, and BAL was performed at 24 h postinfection. BAL fluid samples from 3 or 4 mice were pooled, stained with anti-CD45–APC, and sorted for intracellular cryptococcal cells ($AF488^+$ APC^+; Phag.) or extracellular cryptococcal cells ($AF488^+$ APC^-; Extrac.). The cell concentration after sorting was determined by hemacytometer counts. Cells were plated for viability on YPD medium. Error bars represent standard errors for 2 experiments with 3 or 4 replicate pools.

fungal burdens in the lungs, suggesting that reduced phagocytosis may lead to increased cellular survival.

To test this hypothesis, the viability of *in vivo* phagocytosed and extracellular cryptococcal cells was determined. Mice were infected intranasally with wild-type or *gpr4*Δ *gpr5*Δ cells that had been fluorescently labeled with Alexa Fluor 488 to allow for detection and sorting of the cryptococcal cells. At 24 h postinfection, bronchoalveolar lavages were performed, and samples were stained with anti-CD45–APC to label all phagocytes. Samples were then sorted by FACS, and both phagocytosed cryptococcal cells ($AF488^+$ CD45-APC^+) and extracellular cryptococcal cells ($AF488^+$ CD45-APC^-) were collected. The total cell number in each population was determined during sorting and verified by hemacytometer counting for a subset of samples. The viability of the FACS-sorted populations was determined by comparison of CFU to the total number of cells plated. For the wild-type infections, the viability of the phagocytosed population (12.4%) was significantly lower than the viability of the extracellular population (34.7%) (Fig. 6) ($P = 0.0022$). A similar trend was observed with the *gpr4*Δ *gpr5*Δ strain, which has limited titan cell production ($P = 0.0012$) (data not shown). These results show that phagocytosis of *C. neoformans in vivo* results in decreased cell viability and suggest that reduced phagocytosis in the presence of titan cells decreases killing by phagocytes to promote pulmonary survival.

Titan cell production enhances dissemination of *C. neoformans*. The time course data presented above show that titan cell production promotes survival and proliferation of cryptococcal cells in the pulmonary environment due to decreased phagocytosis. Yet the primary site of disease during cryptococcal infections is the central nervous system (5, 19). Thus, the effect of titan cell production on hematogenous dissemination as well as penetration and replication in the brain was determined.

The number of CFU present in the spleen was used as a measure of the ability of the wild-type and *gpr4*Δ *gpr5*Δ strains to spread hematogenously to other organs. Both the wild-type and *gpr4*Δ *gpr5*Δ strains had no detectable dissemination to the spleen at 7 days postinfection (Fig. 7A). At 14 days postinfection, lower fungal burdens in the spleen were observed for the *gpr4*Δ *gpr5*Δ mutant strain than for the wild type (Fig. 7A). By 21 days postinfection, the *gpr4*Δ *gpr5*Δ mutant strain had a 100-fold reduction in CFU compared to the wild-type strain (Fig. 7A) ($P = 0.01$). These data show that hematogenous dissemination from the lungs is severely impaired in the absence of titan cell production.

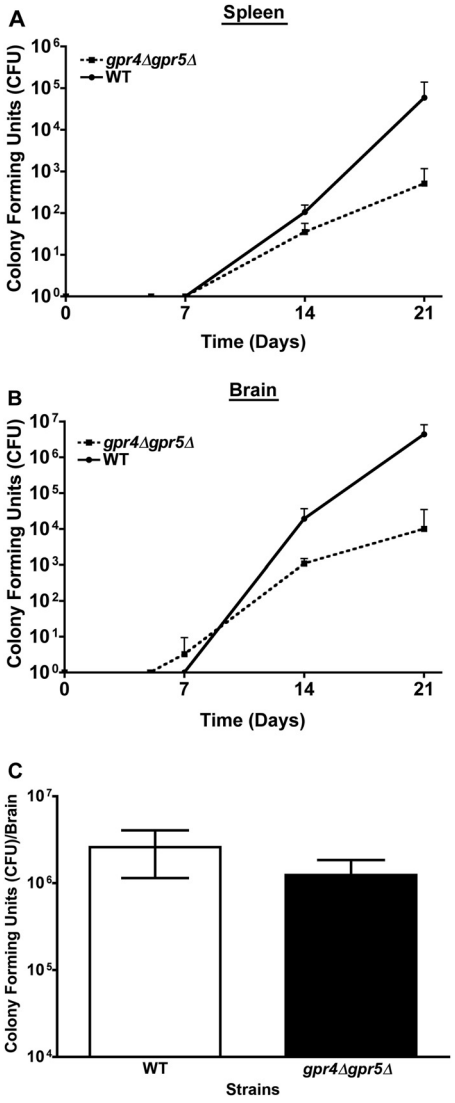

FIG 7 Titan cell production increases dissemination from the lungs. (A and B) C57BL/6 mice were infected intranasally with 1×10^3 wild-type (KN99α) or *gpr4*Δ *gpr5*Δ cells. At 0, 5, 7, 14, and 21 days postinfection, spleens (A) and brains (B) were harvested and homogenized, and serial dilutions were plated for CFU determinations. Error bars represent standard deviations for 7 or 8 mice per strain per time point. (C) C57BL/6 mice were inoculated intracerebrally with 1×10^3 wild-type (KN99α) or *gpr4*Δ *gpr5*Δ cells. At 4 days postinoculation, animals were sacrificed, brains were extracted and homogenized, and serial dilutions were plated for CFU determinations. Error bars indicate standard deviations for 8 mice per treatment group.

Fungal burdens in the brain were also markedly reduced in mice infected with the *gpr4*Δ *gpr5*Δ mutant strain compared to those infected with the wild type (Fig. 7B). Dissemination of the *gpr4*Δ *gpr5*Δ mutant to the brain was higher than that of the wild type at 7 days postinfection, although the difference was not statistically significant (Fig. 7B) ($P = 0.18$). By 21 days postinfection, the *gpr4*Δ *gpr5*Δ mutant strain exhibited a 300-fold decrease in

brain fungal burden compared to that in mice infected with the wild-type strain (Fig. 7B) ($P = 0.001$).

The difference between wild-type and *gpr4*Δ *gpr5*Δ cell accumulation in the brain could be due to reduced survival of the *gpr4*Δ *gpr5*Δ strain in blood, reduced growth of the *gpr4*Δ *gpr5*Δ strain within the brain, or reduced dissemination of the *gpr4*Δ *gpr5*Δ strain. The *gpr4*Δ *gpr5*Δ and wild-type strains had equivalent growth in whole blood (see Fig. S1B in the supplemental material). To examine growth within the brain, mice were infected intracerebrally and CFU were determined at 4 days postinfection. No difference in brain fungal burdens between the *gpr4*Δ *gpr5*Δ and wild-type strains was observed for intracerebral infections (Fig. 7C) ($P = 0.16$). Thus, the wild-type and *gpr4*Δ *gpr5*Δ cells grew equally well in the brain, indicating that the low fungal burdens observed with *gpr4*Δ *gpr5*Δ infection were due to reduced dissemination in the absence of titan cell production.

Titan cell production alters the host immune response. The observation that titan cells enhance multiple aspects of the cryptococcal infectious process, such as growth in the pulmonary environment and dissemination, led us to hypothesize that titan cells are capable of altering the host immune response to promote disease progression. Since eosinophils are recruited to the lung during wild-type infection (36) and play a pathological role in the immune response to *C. neoformans* (21), we compared eosinophil quantities in the lung 14 days after infection with the wild-type strain, which is capable of titan cell production, or the *gpr4*Δ *gpr5*Δ strain, which has minimal titan cell production. Lungs of mice infected with wild-type *Cryptococcus* had larger numbers of eosinophils than did lungs of mice infected with the *gpr4*Δ *gpr5*Δ strain (Fig. 8B) ($P = 0.0256$). In addition, eosinophils accounted for a larger proportion of the host pulmonary immune cell population in mice infected with the wild-type than in those infected with the *gpr4*Δ *gpr5*Δ strain (Fig. 8A) ($P = 0.0013$). Therefore, titan cell production is a potential mechanism that *Cryptococcus* employs to alter host immune responses.

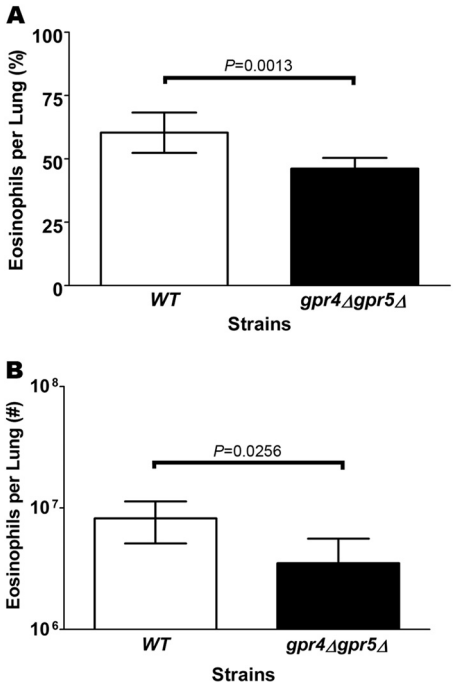

FIG 8 Titan cell production increases eosinophil accumulation in the lungs. Groups of C57BL/6 mice were infected intranasally with 5×10^4 wild-type (KN99α) or *gpr4*Δ *gpr5*Δ cells. Lungs were harvested at 14 days postinfection for enumeration of eosinophils. The proportion of total leukocytes (A) and number of cells per lung (B) that were Siglec-F^+ IgE^- $Ly6G^{int}$ $CD11c^{low}$ are represented. Error bars indicate standard deviations for 4 to 7 mice per group.

DISCUSSION

Virulence factors are phenotypes associated with organisms that promote their pathogenesis. Typically, virulence factors are defined by three criteria: (i) the phenotype is expressed *in vivo*, (ii) the phenotype alters host-pathogen interactions, and (iii) disruption of the phenotype results in altered virulence (17). Titan cells are generated by *C. neoformans* in response to the *in vivo* pulmonary environment, and their production is regulated by the same signal transduction pathway that regulates other known virulence factors (33, 34, 46). The large size of titan cells inhibits phagocytosis by host cells (32, 33, 46). In addition, titan cells exhibit aberrant binding by complement, which likely results in an alteration in the complement-induced host response (46). Titan cells also have characteristics that promote their survival in the host, such as resistance to oxidative/nitrosative stress and structural changes in the capsule and cell wall (33, 46). Thus, titan cells have altered host-pathogen interactions. Using both purified cell populations and mutants with disrupted titan cell production, we show here that titan cell production promotes survival and proliferation in the lungs and dissemination to the brain and ultimately results in enhanced virulence compared to that of a mutant strain lacking titan cell formation. These data unequivocally show that titan cell production has all the hallmarks of a novel virulence factor generated by *C. neoformans* to promote virulence.

Titan cell production is observed predominantly in the lungs and is readily apparent in experimentally infected mice by 24 h postinfection (33). Mice infected with purified titan cells exhibited increased fungal burdens at early time points, showing that titan cells can promote establishment of pulmonary infection. Interestingly, the effect of titan cell production on early pulmonary infections was more pronounced when mice were infected with purified titan cells than when they were infected with mutant strains with altered titan cell formation. These differences were likely due to intrinsic differences in cells of the infecting inoculum because of cell size or tolerance to the host environment.

Resident alveolar macrophages phagocytose and kill inhaled pathogens, but titan cells are too large to be phagocytosed (32, 33). Because titan cells themselves are protected from phagocytosis due to their size (32), the vast majority of the cells in the purified titan cell inoculum would survive the initial host phagocytic immune response, resulting in increased survival. To generate purified cell populations, the cells were passaged in mice to stimulate titan cell production. Thus, the purified cell populations were already acclimated to the host environment. The 10-fold increase in fungal burden in infections with purified titan cells compared to those with purified normal-size cells was likely due to the inability of the resident alveolar macrophages to phagocytose and kill the titan cells. The effect of previous exposure to the host environment was minimized by using purified normal-size cells that had also been passaged through mice.

In contrast, the *gpr4*Δ *gpr5*Δ mutant and wild-type strain in-

oculums were grown *in vitro*. Not only were all of the cells in the infecting inoculums of a normal size, but also the cells were not acclimatized to the host environment. The wild-type and *gpr4*Δ *gpr5*Δ strains exhibited equivalent early cell death upon exposure to the pulmonary environment. The similarity between the wild-type and *gpr4*Δ *gpr5*Δ cell survival rates could be because the cells were not acclimatized to the host environment. The low level of titan cell production in the wild-type strain at early time points may be insufficient to protect the majority of cells in the inoculum from phagocytosis by resident alveolar macrophages. Instead, protection from phagocytosis for the wild-type strain may have a larger impact later in the infection, when additional phagocytic cells are recruited to the lungs.

Our viability data show that in early lung infections, it is not beneficial for *C. neoformans* to be phagocytosed. Increased phagocytosis of the *gpr4*Δ *gpr5*Δ strain at early stages of infection was correlated with lower fungal burdens at later times during infection. These data suggest that an intracellular lifestyle is less conducive to growth and survival of *C. neoformans* than an extracellular lifestyle. There are common features that distinguish extracellular pathogens from intracellular pathogens. Extracellular pathogens employ mechanisms to prevent phagocytosis, are capable of extracellular replication, and are generally thought to prime a humoral immune response. For example, the extracellular pathogen *Streptococcus pyogenes* produces a capsule of hyaluronic acid that aids in prevention of phagocytosis and antibody-mediated opsonization, which is an essential component of protective immunity against *S. pyogenes* (42). Conversely, intracellular pathogens actively stimulate uptake into host cells and utilize mechanisms for intracellular survival and replication, and their clearance requires induction of a cell-mediated immune response. For example, the intracellular pathogen *Listeria monocytogenes* escapes the phagolysosome by using the protein listeriolysin O, allowing *L. monocytogenes* to survive and replicate in the cytoplasmic space of the host cell. *L. monocytogenes* also produces internalins that stimulate entry into host cells (14).

C. neoformans, being a facultative intracellular pathogen, exhibits characteristics of both extracellular and intracellular microorganisms. Like *S. pyogenes*, *C. neoformans* induces production of an antiphagocytic capsule *in vivo* (19). Uptake of cryptococcal cells into phagocytes is not actively induced by cryptococcal factors but rather is due to recognition and subsequent uptake by the phagocyte (19). Once inside the phagolysosome, *C. neoformans* can actively extrude itself from the cell into the extracellular space by nonlytic exocytosis, or vomocytosis (2, 3, 25). Yet, like intracellular pathogens, once *C. neoformans* is taken up by a host phagocyte, it induces production of a large variety of genes that allow for intracellular survival in the phagolysosome (18).

While *Cryptococcus* is able to survive both intracellularly and extracellularly, it appears that titan cell production promotes the extracellular lifestyle by prevention of phagocytosis. The protection from phagocytosis by titan cell production occurs in at least two ways. Titan cells themselves are intrinsically protected from phagocytosis due to their large size (32, 33). Yet titan cell production also has a global effect, because normal-size cells are protected from phagocytosis when titan cells are present (32). This shift toward an extracellular lifestyle aids in better cryptococcal cell survival in the early stages of infection, which is likely essential for establishment of the infection. In addition, the observation that *otc1*Δ cells are not cleared from the lungs for at least 2 months suggests that the host immune response is unable to efficiently kill extracellular titan cells.

The viability of phagocytosed cryptococcal cells was decreased compared to that of extracellular cryptococcal cells. This was somewhat surprising given the evidence that at later stages of infection, intracellular *C. neoformans* promotes dissemination to the CNS (11, 15, 24). These studies create a paradox where in one case an intracellular lifestyle leads to reduced cell viability and is negatively correlated with virulence and in the other case an intracellular lifestyle promotes disease by increasing dissemination to the CNS. Our studies examined phagocytosis at early stages of infection. It is possible that in later stages of the infection, the immune environment is altered such that it is more permissive for intracellular survival and replication. The observation that titan cell production increases the number and proportion of eosinophils in the lungs supports this hypothesis. Eosinophils are typically produced in response to extracellular pathogens and are characteristic of T_H2-type immune responses, where a classical phagocytic response is not as protective. As the cryptococcal infection progresses, changes in the cell types present in the lungs or the activation state of the alveolar macrophages could shift from a classically activated fungicidal state toward an alternatively activated state that is more permissive for intracellular growth. An alternative hypothesis is that fitness of the cryptococcal cells themselves could change over the course of infection. As the cryptococcal cells continue to adapt to the host environment, they may develop better tolerance for the intracellular lifestyle. Previous studies have shown that cryptococcal cells upregulate a number of genes whose protein products are important for survival within macrophages upon phagocytosis *in vitro* (18).

Intracellular cryptococcal cells have increased dissemination to the CNS compared to extracellular cells (11). Thus, the effect that titan cell production had on dissemination of *C. neoformans* to the CNS was surprising. In the absence of titan cells, we anticipated that increased phagocytosis would result in increased dissemination. This could be true, as the *gpr4*Δ *gpr5*Δ mutant cells were detected in the brain earlier than the wild-type cells. However, the overall dissemination was much lower for the *gpr4*Δ *gpr5*Δ mutant than for the wild type. These data suggest that other effects of titan cell production, beyond simply limiting phagocytosis, alter dissemination from the lungs.

Unfortunately, because the *otc1*Δ mutant strain had a replication defect *in vivo*, we were unable to determine the long-term effect of titan cell overproduction on cryptococcal virulence. Previous studies which overproduced titan cells through stimulation of pheromone signaling showed decreased CNS penetration (29). The fact that no dissemination of the *otc1*Δ mutant strain was observed provides further support that titan cells themselves may not be able to exit the lungs. Even though the *otc1*Δ titan cells did not disseminate, the cells were able to persist in the lungs for a minimum of 2 months. Thus, titan cell production may also play a key role in the development of dormant or persistent infections. Evidence suggests that dormant cryptococcal infections that develop in healthy individuals can reactivate upon failure of the immune system (16).

Titan cell production is involved in promoting cryptococcal cell survival, proliferation, and dissemination. Thus, titan cell production plays a key role in cryptococcal virulence and could be a novel target for treatment strategies aimed at reducing infection rates or dissemination in immunocompromised patient popula-

tions. Drug treatments that target developmental or morphological stages important for pathogenesis have been developed for other eukaryotic parasites. In malaria, some drugs target schizonts while other drugs target gametocytes (44). Similarly, drugs that target microfilaria dramatically reduced canine heartworm infections by *Dirofilaria immitis* (27). If similar treatment strategies targeting titan cells are developed for *C. neoformans*, the incidence of these infections and their impact could be reduced dramatically.

ACKNOWLEDGMENTS

We thank Jennifer Blalock, Kyle Smith, Lindsay Nevalainen, Alycia Legeros, and Michelle Goettge for their assistance with experiments. We also thank Dana Davis for helpful comments and discussions. The Flow Cytometry Core Facility at the University of Minnesota was integral in the flow cytometry and cell sorting experiments.

This work was supported by NIH grant AI080275 to K.N. J.N.C. was also supported by a fellowship from the 3M Corporation. L.H.O. was supported by the Dennis W. Watson Fellowship and by a doctoral dissertation fellowship from the University of Minnesota.

REFERENCES

1. **Alspaugh JA, Perfect JR, Heitman J.** 1997. *Cryptococcus neoformans* mating and virulence are regulated by the G-protein alpha subunit GPA1 and cAMP. Genes Dev. **11**:3206–3217.
2. **Alvarez M, Casadevall A.** 2006. Phagosome extrusion and host-cell survival after *Cryptococcus neoformans* phagocytosis by macrophages. Curr. Biol. **16**:2161–2165.
3. **Alvarez M, Casadevall A.** 2007. Cell-to-cell spread and massive vacuole formation after *Cryptococcus neoformans* infection of murine macrophages. BMC Immunol. **8**:16.
4. **Cannon GJ, Swanson JA.** 1992. The macrophage capacity for phagocytosis. J. Cell Sci. **101**:907–913.
5. **Casadevall A, Perfect JR.** 1998. *Cryptococcus neoformans*. ASM Press, Washington, DC.
6. **Chang YC, et al.** 1997. Structure and biological activities of acapsular *Cryptococcus neoformans* 602 complemented with the CAP64 gene. Infect. Immun. **65**:1584–1592.
7. **Chang YC, Kwon-Chung KJ.** 1994. Complementation of a capsule-deficient mutation of *Cryptococcus neoformans* restores its virulence. Mol. Cell. Biol. **14**:4912–4919.
8. **Chang YC, Kwon-Chung KJ.** 1998. Isolation of the third capsule-associated gene, CAP60, required for virulence in *Cryptococcus neoformans*. Infect. Immun. **66**:2230–2236.
9. **Chang YC, Kwon-Chung KJ.** 1999. Isolation, characterization, and localization of a capsule-associated gene, CAP10, of *Cryptococcus neoformans*. J. Bacteriol. **181**:5636–5643.
10. **Chang YC, Penoyer LA, Kwon-Chung KJ.** 1996. The second capsule gene of *Cryptococcus neoformans*, CAP64, is essential for virulence. Infect. Immun. **64**:1977–1983.
11. **Charlier C, et al.** 2009. Evidence of a role for monocytes in dissemination and brain invasion by *Cryptococcus neoformans*. Infect. Immun. **77**:120–127.
12. **Chaskes S, Tyndall RL.** 1975. Pigment production by *Cryptococcus neoformans* from *para*- and *ortho*-diphenols: effect of the nitrogen source. J. Clin. Microbiol. **1**:509–514.
13. **Christensen WB.** 1946. Urea decomposition as a means of differentiating *Proteus* and paracolon cultures from each other and from *Salmonella* and *Shigella* types. J. Bacteriol. **52**:461–466.
14. **Cossart P.** 2011. Illuminating the landscape of host-pathogen interactions with the bacterium *Listeria monocytogenes*. Proc. Natl. Acad. Sci. U. S. A. **108**:19484–19491.
15. **Del Poeta M.** 2004. Role of phagocytosis in the virulence of *Cryptococcus neoformans*. Eukaryot. Cell **3**:1067–1075.
16. **Dromer F, Varma A, Ronin O, Mathoulin S, Dupont B.** 1994. Molecular typing of *Cryptococcus neoformans* serotype D clinical isolates. J. Clin. Microbiol. **32**:2364–2371.
17. **Falkow S.** 1988. Molecular Koch's postulates applied to microbial pathogenicity. Rev. Infect. Dis. **10**(Suppl 2):S274–S276.
18. **Fan W, Kraus PR, Boily MJ, Heitman J.** 2005. *Cryptococcus neoformans* gene expression during murine macrophage infection. Eukaryot. Cell **4**:1420–1433.
19. **Heitman J, Kozel TR, Kwon-Chung KJ, Perfect JR, Casadevall A.** 2011. *Cryptococcus*: from human pathogen to model yeast. ASM Press, Washington, DC.
20. **Hsueh YP, Idnurm A, Heitman J.** 2006. Recombination hotspots flank the *Cryptococcus* mating-type locus: implications for the evolution of a fungal sex chromosome. PLoS Genet. **2**:e184. doi:10.1371/journal.pgen.0020184.
21. **Huffnagle GB, Boyd MB, Street NE, Lipscomb MF.** 1998. IL-5 is required for eosinophil recruitment, crystal deposition, and mononuclear cell recruitment during a pulmonary *Cryptococcus neoformans* infection in genetically susceptible mice (C57BL/6). J. Immunol. **160**:2393–2400.
22. **Jong A, et al.** 2012. Hyaluronic acid receptor CD44 deficiency is associated with decreased *Cryptococcus neoformans* brain infection. J. Biol. Chem. **287**:15298–15306.
23. **Jong A, et al.** 2008. Involvement of human CD44 during *Cryptococcus neoformans* infection of brain microvascular endothelial cells. Cell. Microbiol. **10**:1313–1326.
24. **Luberto C, et al.** 2003. Identification of App1 as a regulator of phagocytosis and virulence of *Cryptococcus neoformans*. J. Clin. Invest. **112**:1080–1094.
25. **Ma H, Croudace JE, Lammas DA, May RC.** 2006. Expulsion of live pathogenic yeast by macrophages. Curr. Biol. **16**:2156–2160.
26. **Macher AM, Bennett JE, Gadek JE, Frank MM.** 1978. Complement depletion in cryptococcal sepsis. J. Immunol. **120**:1686–1690.
27. **McCall JW, Genchi C, Kramer LH, Guerrero J, Venco L.** 2008. Heartworm disease in animals and humans. Adv. Parasitol. **66**:193–285.
28. **Missall TA, Moran JM, Corbett JA, Lodge JK.** 2005. Distinct stress responses of two functional laccases in *Cryptococcus neoformans* are revealed in the absence of the thiol-specific antioxidant Tsa1. Eukaryot. Cell **4**:202–208.
29. **Nielsen K, et al.** 2005. *Cryptococcus neoformans* α strains preferentially disseminate to the central nervous system during coinfection. Infect. Immun. **73**:4922–4933.
30. **Nielsen K, et al.** 2003. Sexual cycle of *Cryptococcus neoformans* var. *grubii* and virulence of congenic **a** and α isolates. Infect. Immun. **71**:4831–4841.
31. **Noverr MC, Williamson PR, Fajardo RS, Huffnagle GB.** 2004. CNLAC1 is required for extrapulmonary dissemination of *Cryptococcus neoformans* but not pulmonary persistence. Infect. Immun. **72**:1693–1699.
32. **Okagaki LH, Nielsen K.** 2012. Titan cells confer protection from phagocytosis in *Cryptococcus neoformans* infections. Eukaryot. Cell **11**:820–826.
33. **Okagaki LH, et al.** 2010. Cryptococcal cell morphology affects host cell interactions and pathogenicity. PLoS Pathog. **6**:e1000953. doi:10.1371/journal.ppat.1000953.
34. **Okagaki LH, et al.** 2011. Cryptococcal titan cell formation is regulated by G-protein signaling in response to multiple stimuli. Eukaryot. Cell **10**:1306–1316.
35. **Olszewski MA, et al.** 2004. Urease expression by *Cryptococcus neoformans* promotes microvascular sequestration, thereby enhancing central nervous system invasion. Am. J. Pathol. **164**:1761–1771.
36. **Osterholzer JJ, et al.** 2009. Cryptococcal urease promotes the accumulation of immature dendritic cells and a non-protective T2 immune response within the lung. Am. J. Pathol. **174**:932–943.
37. **Park BJ, et al.** 2009. Estimation of the current global burden of cryptococcal meningitis among persons living with HIV/AIDS. AIDS **23**:525–530.
38. **Pukkila-Worley R, et al.** 2005. Transcriptional network of multiple capsule and melanin genes governed by the *Cryptococcus neoformans* cyclic AMP cascade. Eukaryot. Cell **4**:190–201.
39. **Rosas AL, et al.** 2000. Synthesis of polymerized melanin by *Cryptococcus neoformans* in infected rodents. Infect. Immun. **68**:2845–2853.
40. **Salas SD, Bennett JE, Kwon-Chung KJ, Perfect JR, Williamson PR.** 1996. Effect of the laccase gene CNLAC1, on virulence of *Cryptococcus neoformans*. J. Exp. Med. **184**:377–386.
41. **Stevens WW, Kim TS, Pujanauski LM, Hao X, Braciale TJ.** 2007. Detection and quantitation of eosinophils in the murine respiratory tract by flow cytometry. J. Immunol. Methods **327**:63–74.
42. **Stollerman GH, Dale JB.** 2008. The importance of the group A Strepto-

coccus capsule in the pathogenesis of human infections: a historical perspective. Clin. Infect. Dis. **46**:1038–1045.
43. **Villena SN, et al.** 2008. Capsular polysaccharides galactoxylomannan and glucuronoxylomannan from *Cryptococcus neoformans* induce macrophage apoptosis mediated by Fas ligand. Cell. Microbiol. **10**: 1274–1285.
44. **Wells TN, Alonso PL, Gutteridge WE.** 2009. New medicines to improve control and contribute to the eradication of malaria. Nat. Rev. Drug Discov. **8**:879–891.
45. **Xue C, Bahn YS, Cox GM, Heitman J.** 2006. G protein-coupled receptor Gpr4 senses amino acids and activates the cAMP-PKA pathway in *Cryptococcus neoformans*. Mol. Biol. Cell **17**:667–679.
46. **Zaragoza O, et al.** 2010. Fungal cell gigantism during mammalian infection. PLoS Pathog. **6**:e1000945. doi:10.1371/journal.ppat.1000945.
47. **Zhang J, et al.** 2005. Isolation of lymphocytes and their innate immune characterizations from liver, intestine, lung and uterus. Cell. Mol. Immunol. **2**:271–280.
48. **Zhang M, et al.** 2007. Defining the *in vivo* function of Siglec-F, a CD33-related Siglec expressed on mouse eosinophils. Blood **109**: 4280–4287.